INEL-94/00090
CONF-950828--24

Improved Methodology for Temperature Predictions in Advanced Reactors

R. G. Ambrosek

Idaho National Engineering Laboratory
Lockheed Idaho Technologies Company
P. O. Box 1625
Idaho Falls, ID 83415-3885

G. S. Chang

Idaho National Engineering Laboratory
Lockheed Idaho Technologies Company
P. O. Box 1625
Idaho Falls, ID 83415-3885

ABSTRACT

Advanced nuclear reactors maximize power and/or flux levels for increased performance levels. One of the challenges is accurate prediction of temperatures in the structural components and experiments. An improved methodology utilizing the computer codes MCNP and ABAQUS has been demonstrated in instrumented experiments at the Advanced Test Reactor. The analytical predictions have shown excellent agreement with the measured results.

INTRODUCTION

Advanced nuclear test reactors, such as the Advanced Neutron Source[1], are being designed to increase their specific power with a resultant increase in flux levels in the core and associated experimental facilities. These reactors are being designed to be inherently safe during accidents resulting from postulated losses in forced convection cooling or rupture of primary coolant piping with a resultant depressurization and loss of coolant. One of the challenges faced by designers and safety analysts is to accurately predict the temperatures in structural components, fuel elements, and experiments during normal and off-normal operation of these nuclear reactors. Efforts to maximize power and/or flux levels require accurate predictions of the reactor environment. Advances in computing capability have resulted in the development of new software and detailed models which provide predictions with greater accuracy, allowing increased performance from the nuclear facilities without degradation of their safety margins.

PREVIOUS METHODOLOGY

The Advanced Test Reactor (ATR)[2] is a nuclear research reactor operated at the Idaho National Engineering Laboratory for testing of fuel and structural materials. There is also some production of special isotopes. Design and operation of experiments in the facility require evaluation of the nuclear heat deposition rates and the resulting heat fluxes and temperature distributions. The heating rate is dependent on neutron interactions, prompt gamma rays, and fission product gamma ray deposition. Until recently the gamma heating rates were predicted using as a basis measurements made in various positions during initial reactor startup using graphite-wall and aluminum-wall ionization chambers. Comparisons were made in the Advanced Test Reactor Critical (ATRC) facility using the thermoluminescent properties of CaF_2:Mn and LiF phosphors.[3] Based on the comparisons, it was concluded that it was reasonable to expect CaF_2:Mn measurements in the ATRC to predict gamma heat values in the ATR within 20 percent of the measured ion chamber data.[4]

Neutron flux levels were predicted from flux wire measurements at a low reactor power or as an integrated flux over time. Generally no consideration was given to changes in experimental configuration or changing reactor operating modes (power splits, outer shim control cylinder rotation patterns, etc.)

The neutron and gamma heating were then used to predict the temperatures in the components being evaluated. Results were generally within $\pm 20\%$ of the measured temperatures.

Many of the experimental irradiations were not instrumented and so there was no direct comparison between measured and predicted temperatures. There was one series of instrumented experiments performed for the light water concept for a New Production Reactor. These experiments indicated heat rates were generally within $\pm 20\%$. There were two instrumented lead experiments which had a larger error and the desired operating temperature range could not be obtained.

FACILITY DESCRIPTION

The ATR has a serpentine fuel arrangement which resembles a four-leaf clover (Figure 1). This arrangement provides five flux traps which are internal and nearly surrounded by fuel and four external flux traps which are partially surrounded by fuel. Each of the five lobes can operate at different power levels with the power split controlled by the outer control cylinder position and

DISCLAIMER

insertion or removal of the neck shim rods. Experiments are placed in the flux traps, and various other locations in the cruciform and beryllium reflector. The specific test positions applicable to this paper are position "B-10" and position "B-12", 3.81 cm diameter holes located in the beryllium reflector behind the east outer flux trap and near the E2-E3 and W2-W3 outer shim control cylinders (OSCC). The partial hafnium sleeve on the OSCC rotates toward the facility during initial rotation and then rotates away as maximum rotation occurs. This change in position of the hafnium sleeve relative to the experiment results in a change in thermal neutron flux levels and changes the gamma heating rates as the gamma rays produced by neutron interactions with the hafnium sleeve change relative location.

METHODOLOGY IMPROVEMENT

Advances in computer software and hardware have made it feasible in terms of both time and cost to perform analyses that predict the heating rates for the specific test materials and configuration, and specific reactor operating configuration, i.e., power split and other experimental facility loadings. The primary computer codes used in recent experimental programs for the ATR are MCNP[5] and ABAQUS.[6]

MCNP is a Monte Carlo continuous-energy, three-dimensional coupled neutron photon radiation transport code. These features make Monte Carlo superior to diffusion theory codes when the fluxes are changing very rapidly in the fuel, moderator, and control regions. MCNP also performs coupled neutron-gamma heating analysis in materials for which heating information is available.

The MCNP code can model extremely complex 3-dimensional geometries, and it is only limited by the computer memory capacity and the time necessary to run such models to achieve the desired uncertainty band. MCNP uses continuous pointwise cross-section data evaluated from the ENDF/B-V library, and all neutron and photon reactions included in the library are accounted for in MCNP calculations. A quarter core model of the ATR was constructed using the MCNP capability for reflecting surfaces in symmetric configurations. This decreases the computational time from that required for a full model since fewer neutrons are required to be tracked to maintain the same track lengths and relative error in the local cells of interest. The major components of the model included the test assembly in the reflector test position, the ten (10) fuel elements composing the reactor quadrant being modeled, the outer shim control cylinders, the neck shims, and the irradiation loops comprising the modeled quadrant.

Generally there were four major tallies used in the MCNP calculations process to provide fast fluence, and reaction rates for target depletion prediction, and heat rates for thermal analysis. The first tally in the model computes the neutron flux (particles/cm^2 per fission neutron) averaged over the target cells. The second tally calculates the cell average reaction rate of interest. The third tally calculates the neutron energy and prompt gamma deposition (Mev/g) averaged over the target cells. Last, the fourth tally uses the power distributions in the core fuel regions from the fixed-source case as photon source distribution probabilities to find the gamma heating in the target compact from fission product decay. The fission product gamma spectrum in Reference (7) was used in the photon-only calculations.

The ABAQUS computer code is a general purpose finite element program. The finite element model data which describe the thermal behavior of the experiment are: the elements, nodes, element properties, material definitions, heating rates and appropriate boundary conditions. The code can be used to solve heat transfer problems with radiation and conduction across gas gaps, with thermal expansion/swelling dimensional changes or with stable dimensions.

The application being reported in this paper considered heat transfer only, with the heating rates, boundary conditions, and gap conductances being provided via the user.

EXPERIMENT DESCRIPTION

The experimental assembly was composed of cylindrical test specimens stacked in a graphite holder. A cross-section of the test assembly is illustrated in Figure 2. There was a gas gap between the specimens and the graphite holder. The graphite was instrumented with thermocouples at three axial locations: near the top of the specimen stack, at the vertical midplane, and near the bottom of the stack.

Outside of the graphite holder was a gas zone which was separated into a downcomer and riser zone by a thin stainless steel cylinder. The mixture of gases (He and Ne or Ar) in this gas zone was varied to provide the desired operating temperatures.

The outermost materials were an aluminum sleeve, hafnium, and stainless steel. The stainless steel acted as the pressure boundary and the hafnium was used to regulate the thermal neutron reaction rate at the target position.

Heat generation in all materials was a combination of neutron, primary gamma, and secondary gamma deposition. The test specimens also had a significant heat source due to neutron interactions with test materials. The magnitude of this heat source was time dependent as a result of material depletion.

RESULTS

The experimental data positions reported in this paper are from two experiment assemblies operated in "B10" and "B12". The locations are in the beryllium reflector in the east and west quadrants of the reactor. The heating rates were calculated for three time points during each reactor cycle: near the beginning, near the time OSCC positions started significant rotation outward, and at the end of cycle.

The heat rate data were then input to ABAQUS with the recorded reactor power and gas mixture data. Temperature predictions at the thermocouple locations were completed and comparisons made to the measured data. In some instances corrections were made to the calculated quadrant power to obtain better correspondence between the predicted and measured results. These corrections generally required reductions in the predicted quadrant power. The corrections were identified to be necessary as a result of differences in operating OSCC positions versus the projected operating conditions.

The results of the analysis are shown in Tables 1 and 2. The results demonstrate that the code combination MCNP and ABAQUS predicted temperatures throughout the experiment with a maximum relative error of ten percent, with the nominal error during the remainder of the cycles being approximately three percent. This includes data from all three axial locations along the length of the experiment. Post irradiation counting of flux wires validated the neutron predictions of MCNP. Measured to predicted values were within the counting error bands of ± 10 percent at a 95 percent confidence, which shows a significant improvement as compared to the previous methodology.

CONCLUSIONS

The MCNP-ABAQUS combination has provided an analysis methodology that can accurately predict temperature performance of experiments/structural materials/fuel elements in a nuclear reactor. Heat generation rates can be provided for neutron interactions, and gamma heating from prompt and fission product decay. Results from this comparison demonstrate accuracies for various conditions that are much better than the prior methodology based on phosphors and ionization chambers.

REFERENCES

1. Advanced Neutron Source, Being Designed by Martin Marietta Energy Systems, Inc., Oak Ridge National Laboratory, Oak Ridge, Tennessee.

2. Advanced Test Reactor, Operated by Lockheed Idaho Technologies Company, at the Idaho National Engineering Laboratory, Idaho Falls, Idaho.

3. F. H. Attix (ed.), "Luminescence Dosimetry," Oak Ridge: USAEC Division of Technical Information Extension, 1967.

4. N. C. Kaufman, et.al., "Reactor Physics Results From Low-Power Measurements in the Advanced Test Reactor, IN-1260 Idaho Nuclear Corporation, February 1969.

5. J. Briesmeister (Editor), "MCNP - A General Monte Carlo Code for Neutron and Photon Transport, Version 3A," LA-7396-M, Rev. 2, September 1986.

6. ABAQUS User's Manual, Volume I and II, Version 4.9 Hibbitt, Karlsson and Sorenson, Inc.

7. E. T. Boulette and W. L. Bunch, "Analysis of ZPPR Shield Experiments: Gamma Distribution, WHAN-FR-13, February 1971.

Work performed for the Department of Energy under DOE contract DE-AC07-94ID13223.

TABLE 1. MEASURED VERSUS CALCULATED TEMPERATURE COMPARISON FOR ATR-2A

Cycle	Region (U/M/L)	Measured Temperature (C)	Calculated Temperature (C)	Temperature Differential (C)	Relative Percent Error	Adjusted Quadrant Power (Percent)	Adjusted Temperature (C)	Temperature Differential (C)	Relative Percent Error
92BB	U	672	723	51	7.0		667	-5	-0.7
	M	719	784	65	8.3	-12.0	727	8	1.1
	L	653	718	65	9.1		665	12	1.8
92BM	U	676	734	58	8.6		681	5	0.7
	M	721	789	68	9.4	-12.0	735	14	1.9
	L	662	726	64	9.7		676	14	2.1
92BE	U	677	722	45	6.6		669	-8	-1.1
	M	717	777	60	8.4	-12.0	723	6	0.8
	L	666	719	53	8.0		669	3	0.5
93AB	U	667	668	1	0.1				
	M	718	716	-2	-0.3				
	L	662	662	0	0.0				
93AM	U	671	699	28	4.2				
	M	717	734	17	2.4				
	L	667	671	4	0.6				
93AE	U	677	697	20	3.0				
	M	719	733	14	1.9				
	L	676	680	4	0.6				
93BB	U	669	701	32	4.8				
	M	717	734	17	2.4				
	L	663	671	8	1.2				
93BM	U	673	696	23	3.4				
	M	719	728	9	1.2				
	L	668	667	-1	-0.1				
93BE	U	673	681	8	1.2				
	M	717	715	-2	-0.3				
	L	671	662	-9	-1.3				
94AB	U	672	719	47	7.0		686	14	2.1
	M	716	752	36	5.0	-8.0	717	1	0.1
	L	670	690	20	3.0		658	-12	-1.8
94AM	U	679	720	41	6.0		687	8	1.2
	M	716	756	40	5.6	-8.0	721	5	0.7
	L	679	704	25	3.7		672	-7	-1.0
94AE	U	680	710	30	4.4		677	-3	-0.4
	M	714	747	33	4.6	-8.0	712	-2	-0.3
	L	683	689	6	0.9		657	-26	-3.8
94BB	U	668	710	42	6.3		677	9	1.3
	M	718	759	41	5.7	-8.0	724	6	0.8
	L	664	700	36	5.4		668	4	0.6
94BM	U	670	721	51	7.6	-8.0	687	17	2.5
	M	714	766	52	7.3		731	17	2.4
	L	668	706	38	5.7		673	5	0.7
94BE	U	682	694	12	1.8				
	M	716	731	15	2.1				
	L	665	681	-4	-0.6				

Table 2. MEASURED VERSUS CALCULATED TEMPERATURE COMPARISON FOR ATR-2B

Cycle	Region (U/M/L)	Measured Temperature (C)	Calculated Temperature (C) Adjusted	Temperature Differential (C)	Relative Percent Error	Adjusted Quadrant Power (Percent)
94BB	U	729	724	5.6	-0.8	
	M	783	784	-1.1	0.1	-11.12
	L	702	719	-17.8	2.5	
94BM	U	736	730	6.1	-0.8	
	M	787	788	-1.1	0.1	-7.55
	L	718	731	-12.8	1.7	
94BE	U	742	729	13.3	-1.8	
	M	785	783	1.7	-0.2	-2.47
	L	730	741	-10.6	1.4	
95AB	U	731	734	-2.8	0.4	
	M	789	789	0.6	-0.1	-1.31
	L	718	737	-18.9	2.6	
95AE	U	733	733	0.6	-0.1	
	M	789	789	0.0	-0.0	-6.77
	L	721	736	-15.0	2.0	
95BB	U	724	723	1.1	-0.2	
	M	784	785	-1.1	0.1	2.26
	L	709	731	-21.1	2.9	
95BM	U	733	736	-3.3	0.5	
	M	785	787	-1.7	0.2	-4.52
	L	721	741	-20.6	2.8	
95BE	U	744	736	8.9	-1.2	
	M	785	786	-1.1	0.1	-0.80
	L	734	749	-15.6	2.1	
96AB	U	738	737	1.1	-0.2	
	M	786	786	0.0	0.0	-12.49
	L	727	740	-12.8	1.7	
96AM	U	753	746	7.2	-1.0	
	M	790	789	1.1	-0.1	-6.48
	L	746	747	-1.7	0.2	
96AE	U	754	748	6.7	-0.9	
	M	788	788	-0.6	0.1	-13.72
	L	751	754	-3.3	0.4	
96BB	U	731	741	-10.6	1.4	
	M	788	788	-0.0	0.0	-10.63
	L	725	742	-17.2	2.3	
96BM	U	738	742	-4.4	0.6	
	M	787	786	1.1	-0.1	-8.19
	L	740	736	-3.9	-0.5	
96BE	U	747	750	-3.3	0.4	
	M	788	787	0.6	-0.1	-13.79
	L	751	755	-4.4	0.6	

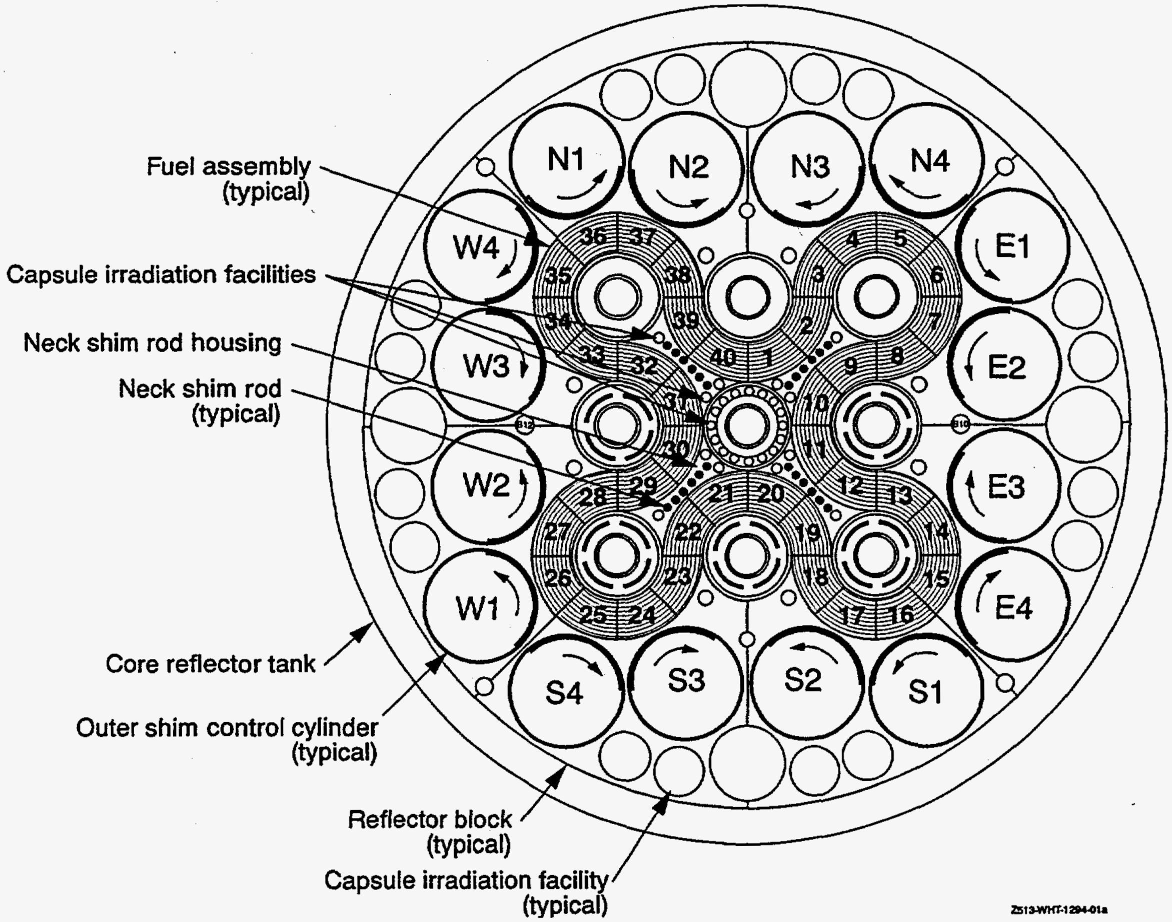

Figure 1. Plan view of ATR core.

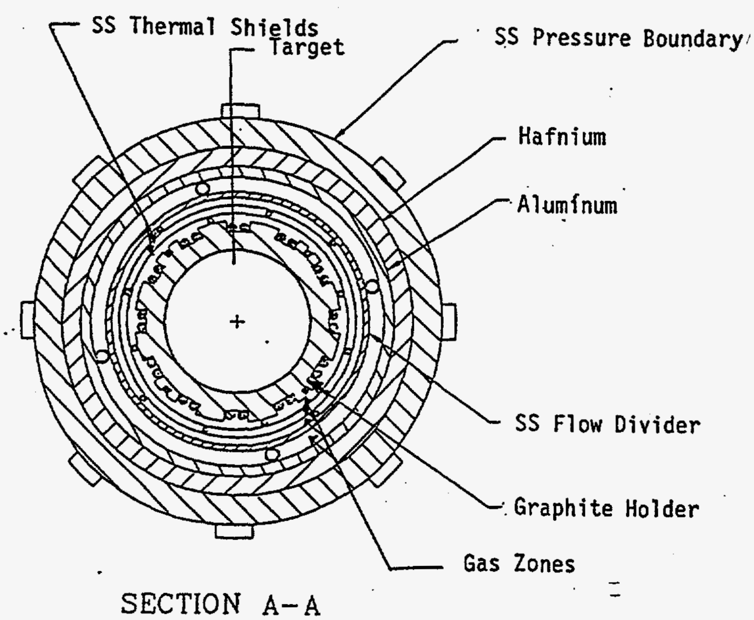

Figure 2. Cross Section of the Test Assembly.